FISEVIER

Contents lists available at ScienceDirect

Photonics and Nanostructures – Fundamentals and Applications

journal homepage: www.elsevier.com/locate/photonics



Manipulating the optical properties of dual implanted Au and Zn nanoparticles in sapphire



E.N. Epie*, D. Scott, W.K. Chu

Physics Department and Texas Center for Superconductivity (TCSUH), University of Houston, TX 77204, USA

ARTICLE INFO

Article history: Received 24 April 2017 Received in revised form 8 August 2017 Accepted 19 September 2017 Available online 25 September 2017

Keywords: Ion implantation Metallic alloy nanoparticles Surface plasmon resonance Sapphire Annealing

ABSTRACT

We have synthesized and manipulated the optical properties of metallic nanoparticles (NPs) by using a combination of low-energy high-fluence dual implantation and thermal annealing. We demonstrated that by implanting Zn before Au, the resulting absorption peak is enormously blue-shifted by 120 nm with respect to that of Au-only implanted samples. This magnitude of optical shift is not characteristic of unalloyed Au and to the best of our knowledge cannot be attributed to NP size change alone. On the other hand, the absorption peak for samples implanted with Au followed by Zn is blue-shifted about 20 nm. Additionally, by carefully annealing all implanted samples, both NP size distribution and corresponding optical properties can be further modified in a controlled manner. We attribute these behaviours to nanoalloy formation. This work provides a direct method for synthesizing and manipulating both the plasmonic and structural properties of metallic alloy NP in various transparent dielectrics for diverse applications.

Published by Elsevier B.V.

1. Introduction

The linear and non-linear optical properties of metallic nanoparticles (NPs) such as gold (Au), silver (Ag), copper (Cu) and aluminium (Al) have made them attractive candidates for diverse applications like the fabrication of ultrafast optical switches [1], optical sensors [2,3], surface enhanced Raman spectroscopy (SERS) [4–7], photocatalysis [8], and ultrasound generators [9,10], to name a few. Gold is particularly interesting because of its chemical stability, a desirable property for sensor applications. Additionally, the intense localised surface plasmon resonance (LSPR) absorption band for Au like Ag and Cu falls within the visible spectrum.

Common methods for synthesizing metallic NPs in various dielectric media include magnetron sputtering, sol-gel deposition, ion exchange, and ion implantation [8,11–13]. Of these, ion implantation is popular because of its versatility [14–16]. Ion implantation allows for high implant filling factors not achievable by other methods, easy controllability, and high precision when it comes to placing implants at the required depth within a matrix. This is achieved by careful control of implantation parameters like ion acceleration voltage and ion fluence. Finally, ion implantation

In spite of the many benefits of ion implantation, the resulting NPs usually present a broad size and spatial distribution which, in some cases, affects their optical properties and may adversely affect the performance of related devices. Such broad size and spatial distributions are due to uncontrolled nucleation and growth processes during implantation, Fig. 1. Some proposed remedies are two-step implantation assisted by intermediate annealing [17], laser annealing [18], posterior ion irradiation [19,20], and dual implantation [21–25]. Of these, dual implantation is attractive because it can lead to the creation of binary compounds or nanoalloys in addition to providing control to the size and spatial distribution of NP implants [8,21]. Furthermore, the resulting nanoalloys may display interesting physical and chemical properties distinct from pure elemental NPs and bulk metals [8,26]. Common implant binaries synthesized so far include, Ag-Cu [27-30], Ag-Au [31,32], Ag-In [33], Ag-Sb [34], Ag-Cd [35].

In a recent study, Wang et al. [21] demonstrated that by dual implanting silica with Zn and Ag ions, the resulting NP size and spatial distribution can be controlled. They further showed that optical properties of the resulting NPs were modified as well. They attributed these optical changes to NP size distribution and Ag-Zn alloy formation. Given that the plasmonic properties of Ag NPs are very sensitive to size [11], a shift in the optical absorption spectrum of Ag + Zn dual implanted samples may not be a sufficient condition

allows us more freedom to select between different implantation substrates.

^{*} Corresponding author.

E-mail addresses: neepie@uh.edu (E.N. Epie), eepien@gmail.com (D. Scott).

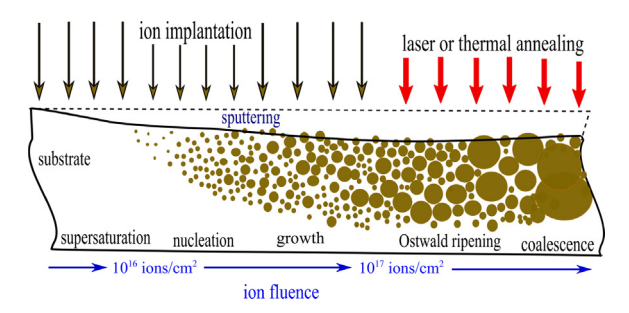


Fig. 1. Schematic illustration of common physical processes involved in nanoparticle formation by ion implantation [11].

for Ag-Zn nanoalloy formation. On the other hand, the plasmonic properties of Au, as compared to Ag, is not very sensitive to NP size as we shall demonstrate. It is therefore important to investigate whether a similar dual implantation technique can produce Au-Zn nanoalloys and what their corresponding optical properties will be.

Using Au and Zn dual ion implantation followed by controlled thermal annealing, we hereby investigate mainly the optical properties of metallic NP implants in sapphire and the associated structural modifications. We demonstrate that, unlike Ag NPs, the plasmonic properties of Au NPs are not very sensitive to size distribution. Interestingly, we observe significant modifications in the size distribution and optical properties of NPs synthesized by Au-Zn dual implantation. Most remarkable is the dependence of NP size and absorption peak position on implantation order and annealing temperature. Using this method, we were able to blue-shift the optical absorption peak of NPs by 120 nm; a shift of this magnitude has never been reported in literature for unalloyed Au NPs, to the best of our knowledge. Therefore, we attribute these behaviours to Au-Zn nanoalloy formation.

It is important to stress here that the primary focus of this paper is on the observed optical modifications. However, it is difficult to talk about these optical changes in isolation. Hence, some preliminary studies on the associated NP structural changes have been presented here to help point us towards possible causes of the observed optical behaviours. An exhaustive study of these structural modifications is ongoing and will be presented in a future article.

2. Experiment

Double-side EPI-polished $10 \times 10 \times 0.43 \, \text{mm}$ slices of Czochralski-grown (MTI Corporation, Richmond, CA) c-plane sapphire with purity >99.99% were dually implanted with 60 keV Au $^-$ and 60 keV ZnO $^-$ ions in different sequences as shown in Table 1. ZnO $^-$ implantation was carried out instead of Zn $^-$ because the beam current obtained for the latter was extremely small, therefore not practical for high fluence implantations [36]. Since we are implanting into an oxide, it makes no difference whether we implant with ZnO $^-$ or Zn $^-$ ions.

The ions used in this study were generated using a *SNICS source* [37,38] and implantations were carried out at room temperature in a high vacuum chamber with partial pressure $P=4 \times 10^{-7}$ Torr. Before implantation, each ion beam was scanned using an elec-

Table 1Sample name and implantation sequence.

Sample name	First implant	Second implant
Au	Au	-
Zn	Zn	_
Au + Zn	Au	Zn
Zn + Au	Zn	Au

trostatic raster scanner to ensure uniformity. During implantation, sample surfaces were slightly tilted off axis to avoid channeling effects and the flux densities for Au $^-$ and ZnO $^-$ ions were maintained at $3.5~\mu\text{A/cm}^2$ and $0.5~\mu\text{A/cm}^2$ respectively. To ensure an equal maximum implant concentration, fluences for implant species were set at $3\times10^{16}~\text{Au/cm}^2$ and $2.5\times10^{16}~\text{ZnO/cm}^2$. After implantation, some samples were annealed for 2~h under Ar in a quartz tube at temperatures between 200~C and 750~C.

Optical absorption spectroscopy and XRD analysis of the resulting nanoparticles were obtained using a *Cary 5000 UV-Vis-NIR spectrophotometer* (Agilent Technologies) and a *D/Max-RA X-ray spectrometer* (Rigaku) respectively. Experimental results were compared with theoretical calculations obtained using *DDSCAT version 7.3.2* [39–41], a robust portable software to calculate scattering and absorption of electromagnetic waves by targets with arbitrary geometries using the discrete-dipole approximation (DDA).

3. Results, analysis and discussions

3.1. Implant concentration profile

At high fluences ($\phi \ge 10^{16} \, \mathrm{cm}^{-2}$), sputtering and ion-beam induced migration of atoms can significantly reduce the implant projected range R_p as shown in Fig. 1. Thus, fluence-dependent depth distribution for implant species can be estimated using the equation [21,42]:

$$G(x,\phi) = \frac{N}{2Y} \left[\text{erf} \left(\frac{x - R_p + \phi Y/N}{\Delta R_p \sqrt{2}} \right) - \text{erf} \left(\frac{x - R_p}{\Delta R_p \sqrt{2}} \right) \right]$$
(1)

where x is the depth coordinate with respect to the instantaneous target (or substrate) surface, N is the atomic density of the substrate, Y is the sputtering yield, ΔR_p is the range straggling related to R_p and "erf()" is the error function. All fitting parameters to Eq. (1) were obtained from computer simulations with the SRIM 2008 [43] code. To simulate Zn distribution, Br was used in SRIM calculations as a model for implanted ZnO. Br was chosen for its close correspondence in atomic mass (79.9 amu) compared to ZnO (81.4 amu). Strictly speaking, therefore, what we consider here as the concentration profile of Zn is more accurately the concentration profile of ZnO ions. However, we do not expect significant differences in the actual profile of Zn.

Fig. 2(a) shows the estimated concentration profile of 60 keV single-ion implanted sapphire, according to Eq. (1). The estimated R_p for 3.0×10^{16} Au/cm² and 2.5×10^{16} Zn/cm² are 8 nm and 18 nm respectively. The maximum concentration of Au ions reaches a saturation value of 10% at fluence $\phi_{Au} = 3.0 \times 10^{16}$ cm⁻² due to the high level of target sputtering during Au implantation. This saturation of Au ions combined with low solute solubility of Au atoms in sapphire, and other factors such as ion induced heat, favours nucleation and growth of Au NPs in sapphire. Larger NPs are mostly found near the sample surface while smaller NPs are concentrated deep beyond R_p . The maximum concentration of Zn ions on the other hand increases with fluence because the sputtering rate of ZnOions is relatively small. Additionally, the diffusivity of Zn interstitials Zn_i is relatively high [44].

In the dual implantation scenarios shown in Fig. 2(b) and (c), the situation is different. In the case where Zn is implanted before Au (Fig. 2(b)), numerical simulations predict R_p for Zn to be 6 nm after Au implantation leading to a significant overlap of Zn and Au profiles. This is due to the high sputtering rate of Au. Although numerical simulations predict no change for Au R_p , since SRIM does not properly account for ion diffusion [43], we expect R_p for Au to be lower than that for Au-only implanted sample. This is because Zn_i will create a depletion layer limiting further diffusion of Au into the substrate. Under these conditions, the maximum concentration of

Download English Version:

https://daneshyari.com/en/article/5449887

Download Persian Version:

https://daneshyari.com/article/5449887

<u>Daneshyari.com</u>